Light Metals 2014
Edited by: John Grandfield
TMS (The Minerals, Metals & Materials Society), 2014

ANODE ROD TO BEAM CONTACT

D. Molenaar and T. Kilpatrick
Commonwealth Scientific and Industrial Research Organisation (CSIRO)
Private Bag 33, Clayton (Melbourne), Victoria, Australia, 3169

Keywords: Contact Resistance, Contact Pressure, Beam-Stem Voltage Drop, Clamp Drop, Anode Assembly

Abstract

The anode rod to beam contact for modern aluminum smelting technology is more sensitive to contact condition than it is to applied force [1]. The contact can consume in excess of 12 kW per cell if not prepared and maintained carefully. There can be significant variation in contact resistance across the contacts on any one cell. Validating improvements of only a few mV for the anode rod to beam contact for operating cells can be very challenging.

The purpose of this paper is to (i) discuss the variation due to measurement technique, and (ii) establish both theoretical and practical benchmarks for common sized connections. The benchmarks presented here are validated against actual plant data measured at several smelters.

Introduction

The authors have had the opportunity to measure the performance of the anode rod to anode beam contact for a wide range of reduction cell technologies at many different smelters over the years. We have noted that for any given type of cell design, there can be a significant variation, not only between smelters, but even between cells and within cells of the same smelter.

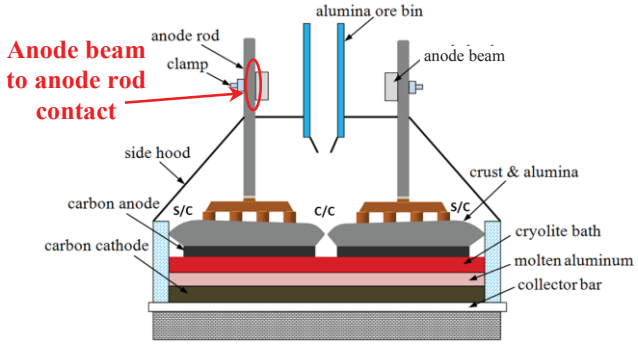

Figure 1. Schematic diagram of an aluminum reduction cell [2] showing the anode rod to anode beam contact.

Recent studies have shown that large aluminum to aluminum high current electrical contacts, such as the anode rod to anode beam connection, Figure 1, are significantly more sensitive to contact condition than to the applied force across the contact [1]. It is commonplace for operations to look for an engineering solution to overcome unnecessarily high contact resistance, such as increasing the clamping force, rather than addressing the more cost effective contact condition. The influence of contact condition is typically grossly underestimated. Several orders of magnitude improvement are possible by improving the surface finish for aluminum to aluminum contacts compared to a doubling of the applied force which, results in only a halving of the contact resistance [3].

Causes of Variation for In-plant Measurements

To eliminate the effect of different reduction cell technologies, in this paper we will concentrate on the AP3x cell technology, which is a popular modern cell technology with many installations around the world. The AP3x cell technology comes in two distinct anode rod sizes and configurations, both of which have been studied here. Collection of detailed clamp voltage drop data has allowed the establishment of a practical industry benchmark by identifying the lowest typical operating points of 10 mV and 12 mV for small and large anode rod to beam configurations, respectively. Figure 2 shows the clamp system voltage drop data from four AP3x smelters; two smelters with 40 small anode rods per cell, and two smelters with 20 large anode rods per cell. Each smelter operates with a line current in the range of 355,000 – 376,000 A DC. As can be seen, the variation in the anode rod to anode beam contact performance can vary considerably between operations of the same technology, and age of the reduction cell. Figure 3 shows the clamp voltage drop data for each anode of one AP3x cell with 40 small anode rods. The data shows clamp drops from 14 – 104 mV with notable variation between left hand side (LHS) and right hand side (RHS) measurements.

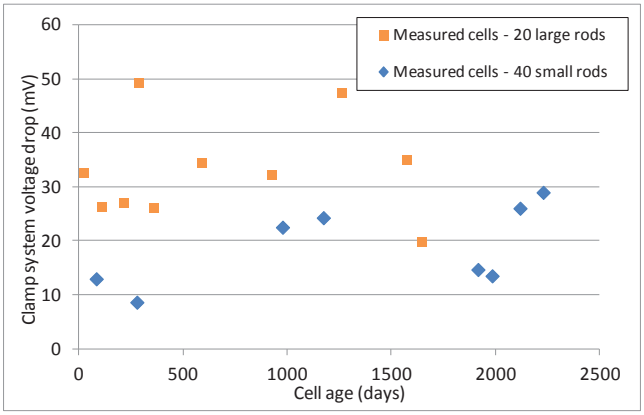

Figure 2. Clamp system voltage drop (mV) as a function of age for AP3x cells with two different anode rod configurations; 40 small or 20 large anode rods per cell.

The most observable problems associated with the anode rod to anode beam contact condition are; loss of contact surface area due to pitting, the formation of raised projections on the anode rod or anode beam contact surface and a buildup of heavy surface oxides and contamination. These are almost always a direct result of stray alumina being present on the anode beam, which makes its way into the anode rod to anode beam contact during setting and beam raising operations, Figure 4. If left unattended it can contribute in excess of an additional 35 mV to total cell voltage drop, Therefore, the elimination of the stray alumina from the anode beam should be the highest priority to minimize subsequent damage to the anode rod and anode beam contact surfaces.

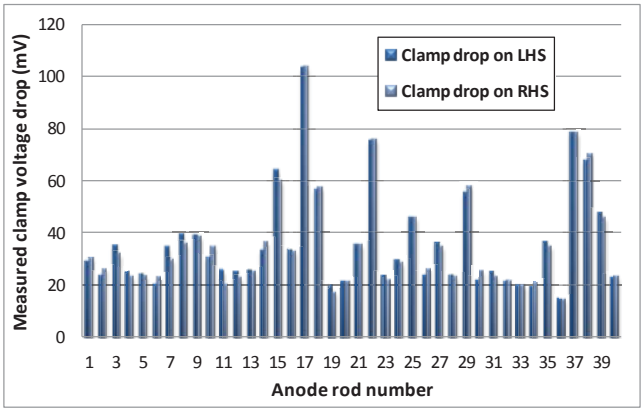

Figure 3. Raw clamp drop voltage data for the anode rod to beam connection (40 small anode rods per cell).

Figure 4. Anode rod clamped in place onto a reduction cell showing stray alumina on top of the anode beam.

Interestingly, not all visible defects need to be repaired. With regards to the repair of pitting damage, it has been shown that only pitting larger than about 22-23 mm in diameter (about the same size as a €1 coin) should be filled and ground back. It is uneconomic and unnecessary to repair all pitting present on the anode rod or anode beam contact face. However, any raised projections on the surface must be removed and made flat by whatever means possible. Cleaning of the anode rod surface each cycle/rota should be undertaken prior to returning any anode rod back to service on a reduction cell [4]. However, it is unfortunately too often observed that rod cleaning devices receive little or no maintenance. For rod brushing systems, the brushes must be replaced at least monthly to remain effective; the economics for this are sound. For rod milling machines, spare cutting blades must be maintained to avoid the unit being placed into bypass.

Other factors in an operating smelter that will affect the performance of the anode rod to anode beam contact performance include;

- Plant layout – i.e. prevailing winds cooling down one reduction line preferentially, or causing more dust problems for a specific reduction line.
- Cell position within the reduction line – i.e. close to the ends where it will be cooler, closer to the offices where it will be monitored/observed more, or proximity to cell feeders where there will inevitably be more of a dusting issue.
- Cell age – newly started cells will generally have lower clamp drop readings because they are cooler and the anode beam should have received appropriate cleaning and maintenance during reconstruction.
- Superstructure age – where the anode beams have undergone years of deterioration including arcing damage, thermal distortion and the buildup of heavy oxides and contamination.
- Stall position – will heavily influence the operating temperature and current draw of the connection. Figure 5 shows a thermal image of an AP3x reduction cell (with 40 small anode rods per cell) and Figure 6 shows the corresponding temperature data measured for both sides of the reduction cell (measured using a contact thermocouple).
- Anode age within the reduction cell – as a function of the initial bath freeze on the underside of a newly set anode, there will be limited current draw for the first few hours of operation. Clearly the rod temperature of newly set anodes will be lower in the first 12-24 hours as the whole assembly heats up after setting, and thus will appear significantly cooler than the other anode rods. Conversely, rod temperatures will be elevated for end of cycle/rota assemblies because they are relatively lower in the cell and are often subjected to being engulfed by cover material, preventing heat loss from the yokes/crossbars.

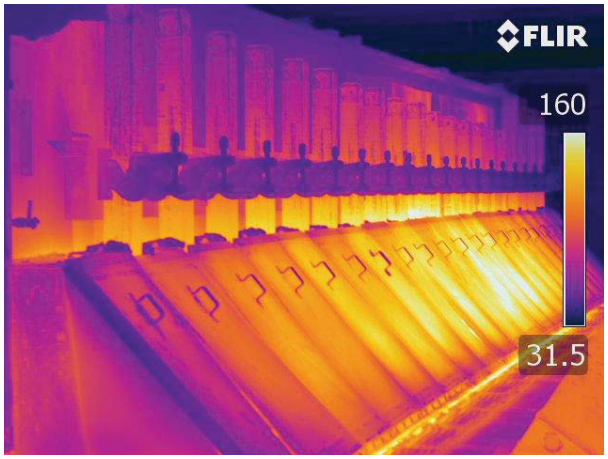

Figure 5. Thermal imaging of reduction cell showing variation of anode rod temperature across the cell.

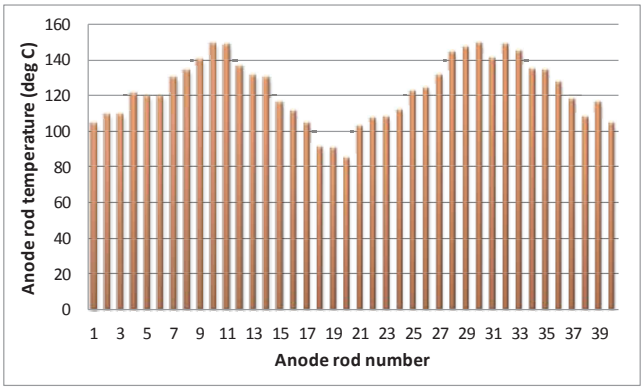

Figure 6. Recorded temperature measurement of anode rods (40 small anode rods per cell).

Often operational staff are applying well intended resources to improve the operating performance of these contacts and are disappointed that the expected improvement is not able to be verified. The problem can usually be overcome by having a detailed knowledge of process variation and utilising the correct measurement technique, which will be different to the measurement technique employed by operations for day-to-day assessments.

This paper focuses on the measurement technique used to verify small improvements in operational voltage drop where there is an extremely large degree of variation. The authors have observed two main methods of measuring the anode rod to anode beam contact voltage drop for AP3x reduction cells; (i) taking the clamp drop measurement from the side of the rod to the front face of the beam as shown in Figure 7, and (ii) taking the measurement from the front face of the rod to the front face of the beam as shown in Figure 8.

Figure 7. Clamp drop measurement from side of rod to front face of beam.

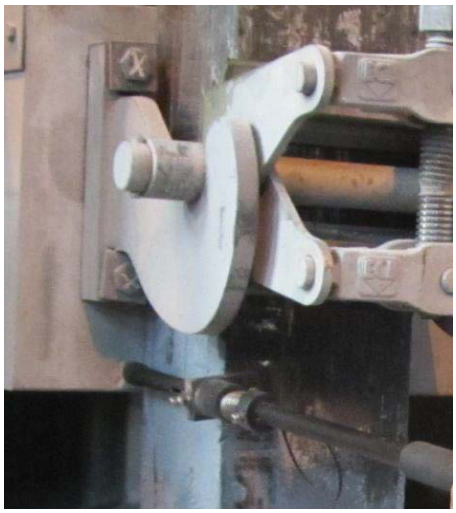

Figure 8. Clamp drop measurement from front face of rod to front face of beam.

Calculation of contact performance must be done in units of resistance, thus it is essential to record the current distribution of each and every anode rod within the cell at the time of the clamp drop measurements. One must also record the actual line current and ensure that the individual rod currents balance with the line current at the time of measurement. The measurement of anode rod current draw is performed as low on the rod as possible above the hood, Figure 9.

Figure 9. Anode rod current draw measurement.

In addition to the anode rod current draw measurement, it is important to measure the temperature of the anode rod to account for changes in material resistivity. This measurement is best performed with a contact thermocouple placed on the side of the anode rod, at a height approximately mid way between the probe points used to measure the anode rod current draw, Figure 10. It has been noted by the authors, through their experience with comparing various types of temperature measurement for anode rods, that the measurement of temperature on the side of the anode rod is far more stable and indicative of actual anode rod temperature, than that measured on the front face of the anode rod.

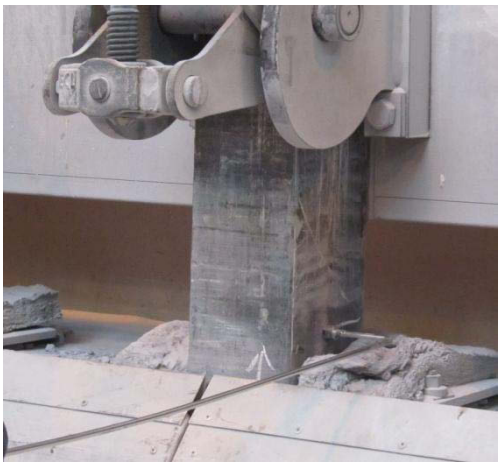

Figure 10. Temperature measurement with contact thermocouple on side of rod.

Theoretical and Practical Benchmarks

A three-dimensional Finite Element Analysis (FEA) model was constructed to study the variation in clamp voltage drop using the two different measurement techniques observed within industry,

for both small (140 × 160 mm) and large (200 × 220 mm) anode rods. The geometry of the models is presented in Figure 11. Variations in current feed to the contact zone exist due to the proximity of each anode rod to the superstructure risers. A range of variations in current feed were studied, Table I, from 100 % current feed within only one side of the anode beam section, to an even 50:50 current feed within both LHS and RHS beam sections. The model was treated as a steady-state coupled thermal-electrical analysis.

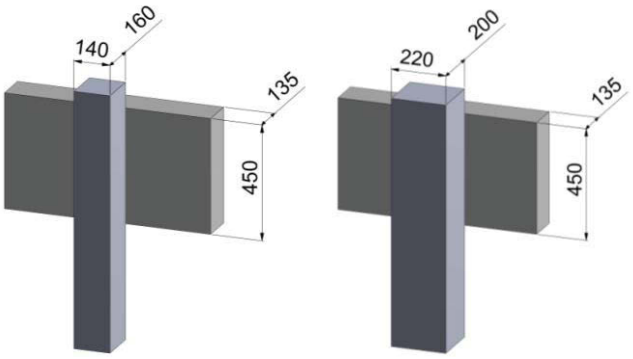

Figure 11. Anode rod and anode beam geometry for both small (left) and large (right) rod configurations. Note: the beam size is constant for the two configurations.

Table I Finite Element Analysis Case Studies

Case	*Rod Size*	*RHS Current Input (A)*	*LHS Current Input (A)*	*Target Clamp Voltage Drop (mV)*
1	Small	9000	-	10
2	Small	6000	3000	10
3	Small	4500	4500	10
4	Large	18000	-	12
5	Large	12000	6000	12
6	Large	9000	9000	12
7	Large	18000	-	40
8	Large	12000	6000	40
9	Large	9000	9000	40

Mesh Statistics

The mesh was constructed in Abaqus/Standard v6.12 using a fully hexahedral mesh discretized with 8-node first-order brick elements (element type DC3D8E). The global edge length of elements was 0.005 m. The mesh statistics are presented in Table II. Figure 12 shows the highly detailed mesh used in the analysis.

Table II Mesh Statistics

Part Description	*Number of Elements*	*Element Type*
Small rod (140 × 160 mm)	179200	DC3D8E
Large rod (200 × 220 mm)	388800	DC3D8E
Beam	352000	DC3D8E

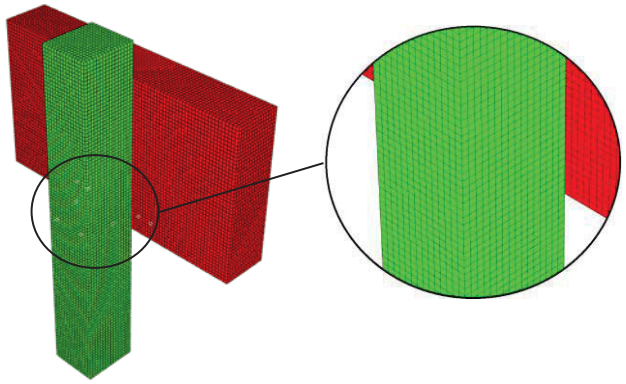

Figure 12. Typical mesh, close-up showing mesh density used (small anode rod configuration shown).

Material Properties

The anode rod material was Al4043 and the anode beam material was Al1350. Temperature dependent material properties were used [5][6].

Operation and Boundary Conditions

During the anode rod to anode beam contact simulation, a constant material temperature of 383 K (110 °C) was applied; representative of the steady-state temperature of the rod to beam connection observed in plant operation. The nodes at the base of both model configurations were prescribed a zero voltage potential, designating that surface as the electrical ground. For Cases 1-6 a contact resistivity of 4.77×10^{-8} Ω.m^2 was used to give an overall clamp voltage drop of 10 mV and 12 mV for the small and large rod to beam connection, respectively. For Cases 7-9 the contact resistivity was increased to 2.02×10^{-7} Ω.m^2 to achieve a clamp voltage drop of approximately 40 mV across the large anode rod to beam configuration, Table III.

Table III Operation and Boundary Conditions

Description	*Value*	*Units*
Total Current density in Small rod (9 kA), where voltage potential is defined as zero.	4.02×10^5	A/m^2
Total Current density in Large rod (18 kA), where voltage potential is defined as zero.	4.09×10^5	A/m^2
Electrical contact conductance from an electrical contact resistivity of 4.77×10^{-8} Ω.m^2 (Case 1 to 6)	2.095×10^7	S/m^2
Electrical contact conductance from an electrical contact resistivity of 2.02×10^{-7} Ω.m^2 (Case 7 to 9)	4.95×10^6	S/m^2
Material temperature: Steady-State	383 (110)	K (°C)

Positions of Probe Sets

Reference nodes on both the anode rod and anode beam were selected to define four 'Probe Sets' at positions that correspond to both LHS and RHS application of the two measurement techniques used by operational staff. The predicted voltage drop was calculated from the voltage potentials at these points, shown in Figure 13 and Figure 14.

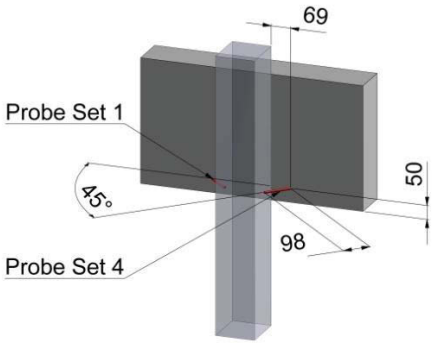

Figure 13. Location of Probe Set 1 (LHS) and Probe Set 4 (RHS).

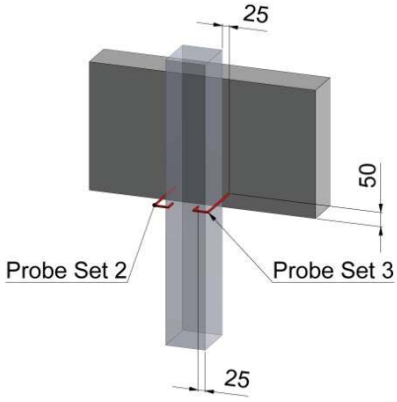

Figure 14. Location of Probe Set 2 (LHS) and Probe Set 3 (RHS).

Results and Discussion

Figure 15 shows the voltage potential (EPOT) distribution for the large anode rod configuration with all of the current being fed from only one side of the beam section (Case 4). In this image each change in colour represents a 2 mV change in voltage potential. With close inspection of the model results, it can be determined that there will be up to a 2 mV difference between measuring LHS and RHS of this configuration.

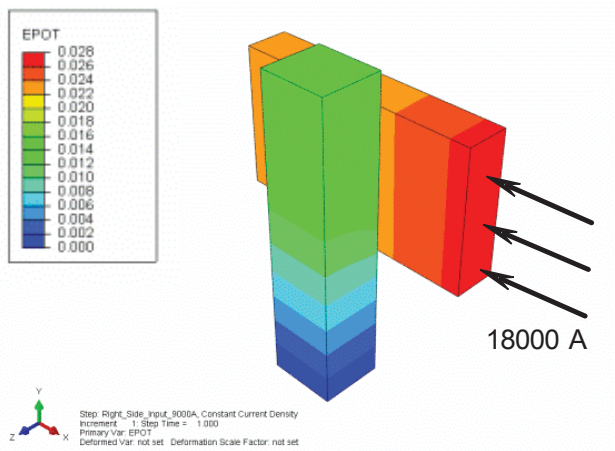

Figure 15. Voltage potential distribution, EPOT (V), across anode rod to anode beam contact showing influence of current feed direction (Case 4, large rod configuration shown).

The theoretical clamp voltage drops for each Probe Set for each case are shown in Figure 16. The results show that the difference in clamp voltage drop between LHS and RHS increases (for either measurement technique) as the current input is biased towards one side of the beam, as would be expected. This is particularly evident for the larger rod configuration (Case 4 and Case 7).

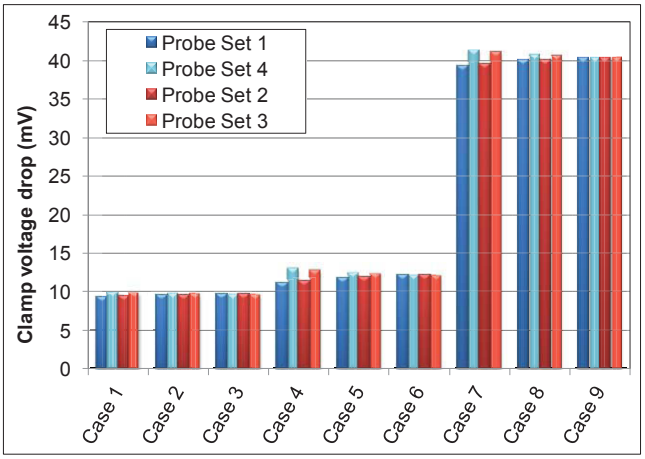

Figure 16. Clamp voltage drop for each Probe Set.

Figure 17 shows the difference in voltage drop between the LHS and RHS for both techniques in more detail. Cases 3, 6 and 9 are zero because the input currents are equal on both sides of the beam. The difference in the voltage drop between the LHS and RHS not only increases as the bias in the current feed increases, but also increases for the larger anode rod configuration, Case 4 and Case 7. Interestingly, the technique measuring from front of anode rod to front of anode beam (Probe Sets 2 & 3) is less sensitive to variation in current feed than the technique measuring at a 45° angle between side of the anode rod and front of the anode beam (Probe Sets 1 & 4).

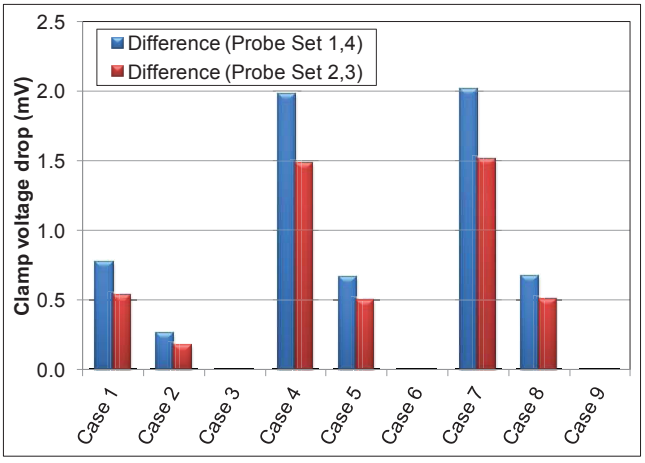

Figure 17. Difference in clamp voltage drop measurements.

An average of the LHS and RHS clamp voltage drop measurements reduces the possibility of inaccurate readings using either technique, especially if these measurements are used to gauge improvements in plant operating procedures of only a few mV. This also means that clamp drop measurements can be compared using either technique, provided you average the results as shown in Figure 18.

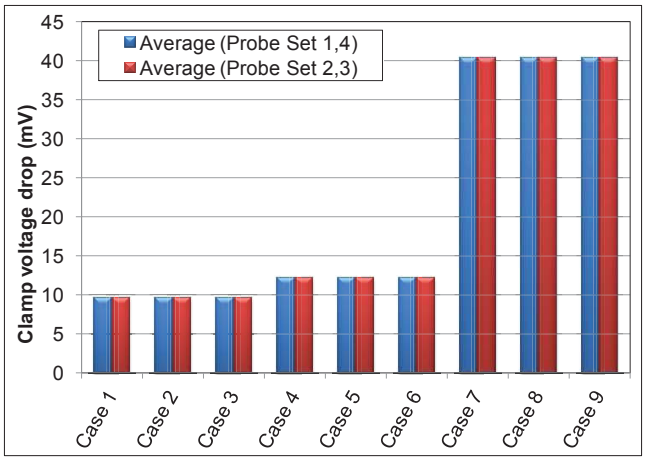

Figure 18. Averaged clamp voltage drop measurements.

The final stage of the analysis was conducted for both anode rod configurations to determine the theoretical voltage drop due to the materials only, i.e. with zero contact resistance. It was found that for both configurations the materials only contribute 1.2-3.0 mV of the measured clamp drop, depending on the anode rod configuration and the current feed arrangement. Therefore it is reasonable to expect that practical industry benchmarks of 10 mV and 12 mV are quite achievable for the small anode rod and large anode rod configurations, respectively.

Concluding Remarks

For the large anode rod configuration, using the diagonal measurement technique on one side only (Probe Set 1 or Probe Set 4) will result in ±1 mV error and should be avoided for validation campaigns trying to confirm improvements of only a few mV across the anode rod to anode beam contact.

Averaging LHS and RHS clamp voltage drop measurements reduces the possibility of inaccurate readings using either technique, especially if these measurements are used to gauge improvements in plant operating procedures. This also means that clamp drop measurements can be compared using either technique provided you average the results.

The practical benchmarks for clamp voltage drop of 10 mV for small anode rod configurations and 12 mV for large anode rod configurations are obtainable for the AP3x technology if contact condition and equipment maintenance factors are addressed, most importantly the elimination of stray alumina from the anode beam in reduction lines and maintenance of anode rod cleaning equipment in rodding rooms.

Acknowledgments

The authors would like to thank CSIRO Minerals Down Under Flagship for financially supporting this work. The authors would also like to thank their numerous clients for providing permission to include various industrial images and data into this manuscript.

References

[1] D. Molenaar, "Use of Electrical Contact Fundamentals in the Aluminium Smelting Industry – A Case Study," *Presented at the 25th International Conference on Electrical Contacts, and 56th Holm Conference on Electrical Contacts, ICEC2010, 2010.*430-438.

[2] K. Ding, D. Molenaar and A. Kapoor, "Prediction of voltage loss on electrical connections for aluminium smelter reduction cells" *Proc. of the Inst. Of Mech. Engrs., Part C, Journal of Mechanical Engineering Science, (2011).* 1-14.

[3] D. Molenaar, "High Amperage Electrical Connections for the Aluminium Smelting Industry" *Masters thesis, Monash University, (2003).*

[4] D. Molenaar, D. Gunasegaram and T. Kilpatrick, "Experimental and numerical studies of surface contamination and degradation of aluminium contacts in primary aluminium smelters" *Presented at the 26th International Conference on Electrical Contacts, ICEC-ICREPEC2012, 2012.* 55-60.

[5] J. R. Davis et. al. (Eds.), ASM Metals Handbook, Vol. 2, Properties and Selection: Nonferrous Alloys and Special-Purpose Materials, *(1990).*

[6] L. Kirkpatrick, Aluminium Electrical Conductor Handbook, Aluminium Association, 3rd Edition, *(1989).*